Magnetically and Biologically Active Bead-Patterned Hydrogels

Daniel C. Pregibon,[†] Mehmet Toner,[‡] and Patrick S. Doyle*,[†]

Department of Chemical Engineering, Massachusetts Institute of Technology, Cambridge, Massachusetts 02139, and Center for Engineering in Medicine, Massachusetts General Hospital, Boston, Massachusetts 02114

Received December 22, 2005. In Final Form: February 27, 2006

We present a new approach to the direct patterning of biologically and magnetically active microbeads in nonbiofouling polymer scaffolds for use in microfluidic devices. Briefly, the process involves treatment of a glass substrate, conformal contact bonding of a PDMS microchannel on the substrate, filling of the channel with beads and prepolymer solution, and UV-initiated photopolymerization of a mask-defined pattern using a standard inverted microscope. This versatile and simple method allows for the rapid fabrication of dispersed or packed bead patterns in poly(ethylene glycol) (PEG) hydrogels that are covalently linked to glass surfaces. By exploiting the relative opacity of the microbeads used, we are able to create both partially exposed and fully encapsulated bead patterns. To demonstrate the utility of this new technology, we separated magnetic bead-bound B lymphocytes from T lymphocytes on a PEG-encapsulated magnetic filtration platform and also captured B cells directly on patterned, protein-decorated beads in a flow-through microfluidic device. Beyond cell sorting, the accurate patterning of industrially standardized, chemically diverse microbeads may have significant implications for microchip-based analyte detection.

Introduction

The ability to pattern magnetic and/or biologically active microbeads in a bioinert environment has important implications for the development of diagnostic, therapeutic, and basic science tools for lab-on-a-chip technologies. Microbeads suspended in aqueous solutions are commonly used in microfluidic devices for chemical reaction and cell binding because of their excellent specificity, wide availability, and appreciable monodispersity. In addition to being industrially standardized, microbeads are available with several protein, electrostatic, or reactive coatings and range in size from hundreds of nanometers to several micrometers. Methods for the precise manipulation and positioning of microbeads (or bead-bound biological targets) on the microscale may have a significant impact on the development of new medical devices.

Microbead patterns are of interest for creating microlense arrays, optical materials, biosensor arrays, and substrates for protein coupling. Traditional techniques employed in patterning colloids on substrates include polymer stamping,[1,2] optical[3−5] or dielectric[6] manipulation, assembly on hydrophilic regions using capillary forces,[7,8] aggregation on patterned silane layers,[9] assembly on physical templates,[10,11] and positioning using scanning electron microscopy.[12] In general, the current bead-patterning technologies are imprecise and leave unstable patterns that can be easily disrupted upon drying or fluid shear stresses. In addition, wet stamping allows the use of only electrostatically charged particles and leaves behind charged polymer residue that must be shielded before device use. Also, these technologies do not permit the direct patterning of biologically active microbeads that require no additional chemical modification prior to analyte capture. Beyond patterning applications, microbeads are commonly used in microfluidic devices for cell sorting,[13,14] immunoassays,[15−17] and DNA hybridization.[18,19] Quite often, magnetic beads are utilized because they can be addressed independently of all other nonmagnetic species.

Paramagnetic, ferromagnetic, and electromagnetic components are commonly used in microfluidic devices to capture or manipulate magnetic species. Magnetic patterns can be accomplished by the electrodeposition of metals through a stencil[20] or onto an etched substrate with subsequent polishing of excess metals.[13] Other methods include the patterning of magnetic microbeads on polymer-stamped regions[21] and micromolding with magnetic-doped poly(dimethyl siloxane).[22] Although these processes yield precise magnetic patterns, they require expensive equipment and timely processes, and the resulting devices

* Corresponding author. E-mail: pdoyle@mit.edu. Phone: (617) 253-4534. Fax: (617) 258-5042.

[†] Massachusetts Institute of Technology.

[‡] Massachusetts General Hospital.

(1) Chen, K. M.; Jiang, X. P.; Kimerling, L. C.; Hammond, P. T. *Langmuir* **2000**, *16*, 7825−7834.

(2) Aizenberg, J.; Braun, P. V.; Wiltzius, P. *Phys. Rev. Lett.* **2000**, *84*, 2997−3000.

(3) Mio, C.; Marr, D. W. M. *Langmuir* **1999**, *15*, 8565−8568.

(4) Won, J.; Inaba, T.; Masuhara, H.; Fujiwara, H.; Sasaki, K.; Miyawaki, S.; Sato, S. *Appl. Phys. Lett.* **1999**, *75*, 1506−1508.

(5) Hoogenboom, J. P.; Vossen, D. L. J.; Faivre-Moskalenko, C.; Dogterom, M.; van Blaaderen, A. *Appl. Phys. Lett.* **2002**, *80*, 4828−4830.

(6) Suzuki, M.; Yasukawa, T.; Mase, Y.; Oyamatsu, D.; Shiku, H.; Matsue, T. *Langmuir* **2004**, *20*, 11005−11011.

(7) Fan, F. Q.; Stebe, K. J. *Langmuir* **2004**, *20*, 3062−3067.

(8) Fustin, C. A.; Glasser, G.; Spiess, H. W.; Jonas, U. *Langmuir* **2004**, *20*, 9114−9123.

(9) Jonas, U.; del Campo, A.; Kruger, C.; Glasser, G.; Boos, D. *Proc. Natl. Acad. Sci. U.S.A.* **2002**, *99*, 5034−5039.

(10) Yin, Y. D.; Lu, Y.; Gates, B.; Xia, Y. N. *J. Am. Chem. Soc.* **2001**, *123*, 8718−8729.

(11) Schaak, R. E.; Cable, R. E.; Leonard, B. M.; Norris, B. C. *Langmuir* **2004**, *20*, 7293−7297.

(12) Miyazaki, H. T.; Miyazaki, H.; Ohtaka, K.; Sato, T. *J. Appl. Phys.* **2000**, *87*, 7152−7158.

(13) Inglis, D. W.; Riehn, R.; Austin, R. H.; Sturm, J. C. *Appl. Phys. Lett.* **2004**, *85*, 5093−5095.

(14) Furdui, V. I.; Harrison, D. J. *Lab Chip* **2004**, *4*, 614−618.

(15) Kim, K. S.; Park, J. K. *Lab Chip* **2005**, *5*, 657−664.

(16) Roos, P.; Skinner, C. D. *Analyst* **2003**, *128*, 527−531.

(17) Choi, J. W.; Oh, K. W.; Thomas, J. H.; Heineman, W. R.; Halsall, H. B.; Nevin, J. H.; Helmicki, A. J.; Henderson, H. T.; Ahn, C. H. *Lab Chip* **2002**, *2*, 27−30.

(18) Fan, Z. H.; Mangru, S.; Granzow, R.; Heaney, P.; Ho, W.; Dong, Q. P.; Kumar, R. *Anal. Chem.* **1999**, *71*, 4851−4859.

(19) Ali, M. F.; Kirby, R.; Goodey, A. P.; Rodriguez, M. D.; Ellington, A. D.; Neikirk, D. P.; McDevitt, J. T. *Anal. Chem.* **2003**, *75*, 4732−4739.

(20) Deng, T.; Prentiss, M.; Whitesides, G. M. *Appl. Phys. Lett.* **2002**, *80*, 461−463.

(21) Lyles, B. F.; Terrot, M. S.; Hammond, P. T.; Gast, A. P. *Langmuir* **2004**, *20*, 3028−3031.

(22) Campbell, C. J.; Grzybowski, B. A. *Philos. Trans. R. Soc. London, Ser. A* **2004**, *362*, 1069−1086.

10.1021/la0534625 CCC: $33.50
Published on Web 04/12/2006

subsequently need to be rendered bioinert for use in most biological applications. Protein-adhesive ligands and protein-resistant polymers are commonly used to modify microdevices for this purpose, defining bioadherent and inert regions.

Spatially controlling the immobilization of proteins is valuable for developing immunoassays, protein microarrays, and cellular arrays for biosensor applications. Several techniques exist for patterning proteins, including deposition using 3D microfluidic systems,[23] photochemical or pH-sensitive deprotection of protein-adhesive substrate coatings,[24,25] polymer-on-polymer stamping,[26] plasma etching using a stamp with subsequent blocking or protein deposition,[27] and chemical vapor deposition polymerization.[28] Microbeads adhered to gold[29] or polyelectrolyte[30] substrates have also been used as solid substrates for protein coupling and subsequent cell culture. Whereas proteins can be used to designate regions for cell attachment, nonbiofouling polymers such as poly(ethylene glycol) can be used to define regions devoid of cells.

Bioinert substrates provide a favorable environment that is chemically transparent to biological species; inert structures often define physical boundaries for cells and proteins but at the same time are resistant to adsorption. Hydrogels are biofriendly, 3D structures that characteristically retain water. Researchers have used UV-polymerizable hydrogels in microfluidics to fabricate stimuli-sensitive valves and pistons[31] as well as scaffolds for cellular arrays.[32,33] Three-dimensional heterogeneous cell arrays have also been realized by polymerizing hydrogels around living cells.[34]

Better methods for patterning biologically and magnetically active components for use in microfluidic environments will have significant implications for the advancement of current lab-on-a-chip technologies. For this purpose, we have developed a method to pattern both magnetic material and proteins in a bioinert polymer using the photopolymerization of bead-containing hydrogel precursors. As such, our approach combines patterning and passivation into a single process. Additionally, the simple method that we present requires minimal reagents and only around an hour to complete and results in stable patterns that are covalently linked to glass substrates.

Materials and Methods

Fabrication of Microfluidic Channels. Microfluidic channels were molded on 4 in. silicon wafers using soft lithography with SU-8 photoresists. Briefly, an SU-8 photoresist (MicroChem) was spin coated on a clean silicon wafer for 30 s at a speed selected to obtain the desired layer thickness. After a brief 65 °C prebake on a hotplate, the wafer was exposed to UV radiation through a transparency mask. The photoresist was then postbaked at 95 °C; subsequently, unexposed photoresist was removed using a developer. Poly(dimethylsiloxane) (PDMS) elastomer (Sylgard 184, Dow Corning) was mixed at a base/curing agent ratio of 1:10. The elastomer was degassed for 30 min and poured over the silicon wafer mold. The PDMS was then cured overnight at 65 °C, and the PDMS mold was peeled from the wafer and individual channels were cut out using a scalpel. Holes for syringe connection were punched out using a blunt-end syringe needle, and wells were cut at the end of the channels using a scalpel. The channels were sonicated in ethanol and rinsed with water prior to use to remove any debris or dust.

Treatment of Glass Substrates. Glass slides (VWR, 24 × 60 mm^2) were soaked in 1 M sodium hydroxide for at least 30 min prior to use. The slides were rinsed thoroughly with deionized water, dried under argon, and treated with oxygen plasma for 90 s. In a 6 mL vial, a solution of 2% methacryloxypropyl trimethoxysilane (MPTMS, Sigma) in pH 5 ethanol was prepared and allowed to hydrolyze for 5 min. In a plastic Petri dish, 250 μL of the MPTMS solution was pipetted onto each clean glass slide and rocked back and forth for 3 min to ensure homogeneous coverage. Slides were held upright, and excess MPTMS solution was dabbed off the bottom edges using an absorbent towel. Each slide was then dipped briefly in ethanol to remove unbound MPTMS. The slides were placed on a hotplate in a glass Petri dish at 75 °C for 15 min to cure. Then the slides were rinsed thoroughly with ethanol followed by deionized water and dried under argon.

Microscope Configuration. All experiments were performed using an Axiovert200 (Zeiss) inverted microscope with a VS25 shutter system (UniBlitz) in place to control the UV exposure dose precisely. A 100 W HBO mercury lamp in conjunction with a wide-range excitation UV filter (11000v2:UV, Chroma) provided radiation of the desired wavelength. Transparency masks designed using Autocad were printed by CAD/Art Services, Inc. (Poway, CA) at 10 000 dpi resolution. Each mask was designed to be circular, 2.5 cm in diameter, with features typically printed no more then 0.5 cm radially from the center of the mask. During an experiment, a mask was sandwiched between two 18 × 18 mm^2 glass coverslips, placed in the first slot of the filter slider bar, and secured with an O-ring. The filter slider was then positioned in the field-stop position of the microscope. Images were processed using NIH Image. The shutter system was controlled using a VMM-D1 shutter driver (UniBlitz), which was prompted using a macro written in NIH Image.

Cell Culture. Raji B and Molt-3 T cells (both from ATCC) were cultured in 150 cm^2 tissue culture flasks in an incubator adjusted to 5% CO_2/95% air at 37 °C. The cells were incubated in RPMI-1640 media supplemented with 10% fetal bovine serum and 200 U/mL penicillin. Prior to use, the cells were centrifuged at 150*g* for 5 min. After aspirating excess media, the cells were resuspended in phosphate-buffered saline containing 0.1% bovine serum albumin (BSA) and 2 mM EDTA (both OmniPur).

Bead-Patterned Hydrogel Materials. Hydrogels were polymerized using solutions of poly(ethylene glycol) diacrylate (PEG-DA, n = 400, Polysciences) with up to 2.5% 2-hydroxy-4′-(2-hydroxyethoxy)-2-methylpropiophenone (HHEMPP, Aldrich, tradename Irgacure 2959) photoinitiator, 33% PBS (Invitrogen), and 1% surfactant. We used Dynabeads M-450 epoxy (4.5 μm, Dynal) with 1% Tergitol NP-10 (Sigma) surfactant to generate magnetic patterns and Dynabeads CD19 (4.5 μm, Dynal) in 1% Tween-20 surfactant (Teknova) to generate protein-bound bead patterns. Protein-coated beads were rinsed with a solution of 10% BSA in PBS during the patterning process.

Results and Discussion

We demonstrate a simple technique to fabricate intricate monolayer patterns of paramagnetic and antibody-decorated microbeads on glass substrates via photopolymerization using a standard inverted microscope. Our approach provides a simple, inexpensive, versatile method for generating free-standing or poly(ethylene glycol)-surrounded magnetic and biologically active patterns. Using magnetic and fluid forces, we demonstrate the ability to pattern self-assembled, dispersed-bead patterns and

(23) Chiu, D. T.; Jeon, N. L.; Huang, S.; Kane, R. S.; Wargo, C. J.; Choi, I. S.; Ingber, D. E.; Whitesides, G. M. *Proc. Natl. Acad. Sci. U.S.A.* **2000**, *97*, 2408−2413.
(24) Dillmore, W. S.; Yousaf, M. N.; Mrksich, M. *Langmuir* **2004**, *20*, 7223−7231.
(25) Christman, K. L.; Maynard, H. D. *Langmuir* **2005**, *21*, 8389−8393.
(26) Kim, H.; Doh, J.; Irvine, D. J.; Cohen, R. E.; Hammond, P. T. *Biomacromolecules* **2004**, *5*, 822−827.
(27) Khademhosseini, A.; Suh, K. Y.; Jon, S.; Eng, G.; Yeh, J.; Chen, G. J.; Langer, R. *Anal. Chem.* **2004**, *76*, 3675−3681.
(28) Lahann, J.; Balcells, M.; Rodon, T.; Lee, J.; Choi, I. S.; Jensen, K. F.; Langer, R. *Langmuir* **2002**, *18*, 2117−2122.
(29) Gleason, N. J.; Nodes, C. J.; Higham, E. M.; Guckert, N.; Aksay, I. A.; Schwarzbauer, J. E.; Carbeck, J. D. *Langmuir* **2003**, *19*, 513−518.
(30) Zheng, H. P.; Berg, M. C.; Rubner, M. F.; Hammond, P. T. *Langmuir* **2004**, *20*, 7215−7222.
(31) Beebe, D. J.; Moore, J. S.; Bauer, J. M.; Yu, Q.; Liu, R. H.; Devadoss, C.; Jo, B. H. *Nature* **2000**, *404*, 588−590.
(32) Folch, A.; Jo, B. H.; Hurtado, O.; Beebe, D. J.; Toner, M. *J Biomed. Mater. Res.* **2000**, *52*, 346−353.
(33) Khademhosseini, A.; Yeh, J.; Jon, S.; Eng, G.; Suh, K. Y.; Burdick, J. A.; Langer, R. *Lab Chip* **2004**, *4*, 425−430.
(34) Liu, V. A.; Bhatia, S. N. *Biomed. Microdevices* **2002**, *4*, 257−266.

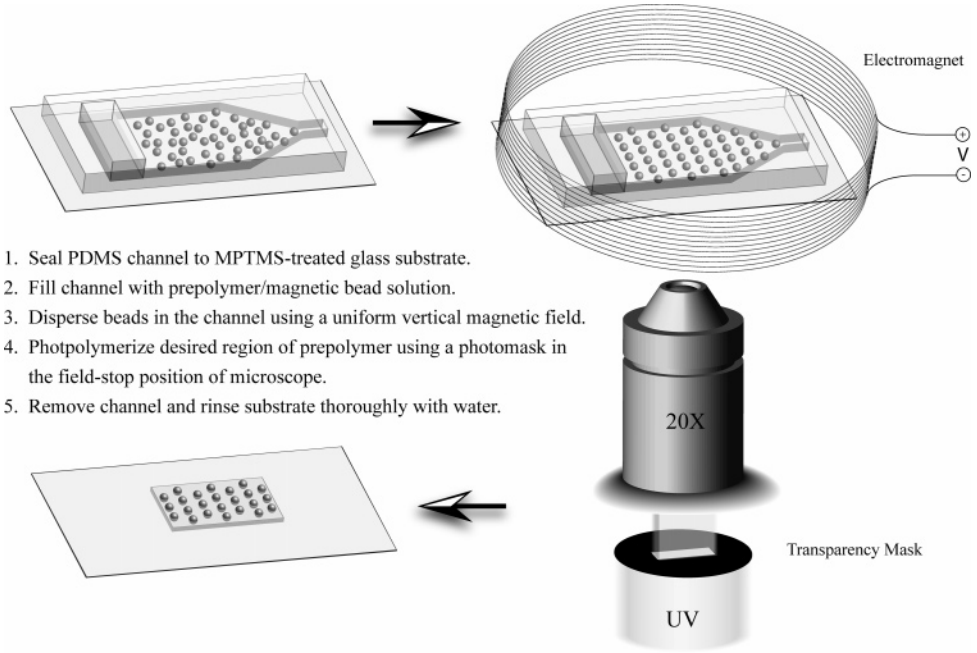

Figure 1. Schematic diagram of structure polymerization for dispersed magnetic bead patterns.

also close-packed bead patterns. The scheme we use for polymerization is similar to that demonstrated by Love et al.[35] This microscope-based projection lithography, which we employed with a 20× objective (providing an overall 7.78× reduction of feature sizes printed on our masks), allows us to fabricate structures over regions greater than 1×1 mm^2 with resolution near 1 μm using repeated short-dose pulsing.

Principles of Patterning. Bead-embedded PEG microstructures were fabricated by photopolymerizing mixtures of beads and UV-sensitive prepolymer in low-height channels that were 9.6 μm tall for disperse-bead patterns or 6.1 μm tall for packed patterns. A schematic of the patterning protocol that we have developed for creating dispersed patterns is shown in Figure 1; the method is discussed in more detail later. We postulate that during the free-radical reaction the bifunctional PEG molecules covalently link with the methacrylate-treated glass substrate and also interact with the microbeads either by means of molecular entanglement or chemical linkage, rendering the beads immobilized on the substrate. Once the primary bead pattern is polymerized to the substrate, the surface can be rinsed and secondary patterns of beads or PEG can be deposited.

It is very important to account for the diffusion of oxygen through PDMS when polymerizing low-profile (less than 10 μm) structures as we have. Oxygen is known to inhibit free-radical polymerization.[36] During the cross-linking reaction, oxygen diffuses rapidly through the PDMS walls and into the monomer, necessitating the use of a relatively high concentration of photoinitiator (or excitation) when polymerizing thin films. Under the conditions that we use, there is always an unreacted liquid "inhibition layer" near the PDMS surface. We have visually confirmed the presence of this inhibition layer near PDMS sidewalls by UV-exposing regions that extend beyond the width of an oligomer-filled channel (data not shown). Similar results are observed when UV exposing across an oligomer/air bubble interface, thus supporting the proposed mechanism of oxygen inhibition.

Because of this phenomenon, we postulate that polymerization is always initiated from the glass surface (where oxygen must diffuse the furthest) and proceeds toward PDMS to a height that is dependent on initiator concentration, UV intensity, and exposure duration.[37] To validate this postulation, we polymerized PEG structures at various doses of UV radiation both through the glass substrate and also through the PDMS as shown in Figure 2. Using a precursor solution of 2.5% HHEMPP photoinitiator in PEG-DA oligomer, we show that the heights of the square structures asymptotically approach a value near 9 μm (in a channel 9.6 μm tall) with increasing exposure dose. Most importantly, the structures were similar in height, regardless of irradiation direction (through glass or PDMS). We have also demonstrated that the structure heights approached different values when the amount of photoinitiator or the UV intensity was altered (not shown).

Beyond controlling structure height, we also exploit the opacity of the beads used to generate patterns of beads whose surfaces are exposed in a PEG platform. Thus, by varying the direction of polymerization (i.e., through the glass or through the PDMS channel), we can generate exposed or totally encapsulated bead patterns. We have patterned encapsulated magnetic microbeads as well as exposed protein-decorated microbeads in order to perform different functions in microfluidic devices.

Dispersed-Bead Magnetic Patterns. We used the self-assembly of colloidal monolayers in a homogeneous magnetic field to generate patterns of paramagnetic microbeads semi-regularly dispersed in PEG hydrogels. The protocol for fabricating a dispersed-bead pattern is outlined in Figure 1 as mentioned before. Briefly, we treated a glass slide with MPTMS (as previously described), bonded a wide, 9.6-μm-tall PDMS channel to the treated glass by conformal contact, filled the channel with prepolymer solution (Dynabeads M-450 epoxy suspended in 2.5% HHEMPP/1% Tergitol NP-10/96.5% PEG-DA) using capillary action, dispersed the beads using an electromagnet-generated vertical magnetic field (10−30 mT), and polymerized mask-defined shapes using a 20× microscope objective for 0.5−3 s.

(35) Love, J. C.; Wolfe, D. B.; Jacobs, H. O.; Whitesides, G. M. *Langmuir* **2001**, *17*, 6005−6012.
(36) Decker, C.; Jenkins, A. D. *Macromolecules* **1985**, *18*, 1241−1244.
(37) Dendukuri, D.; Pregibon, D. C.; Collins, J.; Hatton, T. A.; Doyle, P. S. *Nat. Mater.*, accepted for publication.

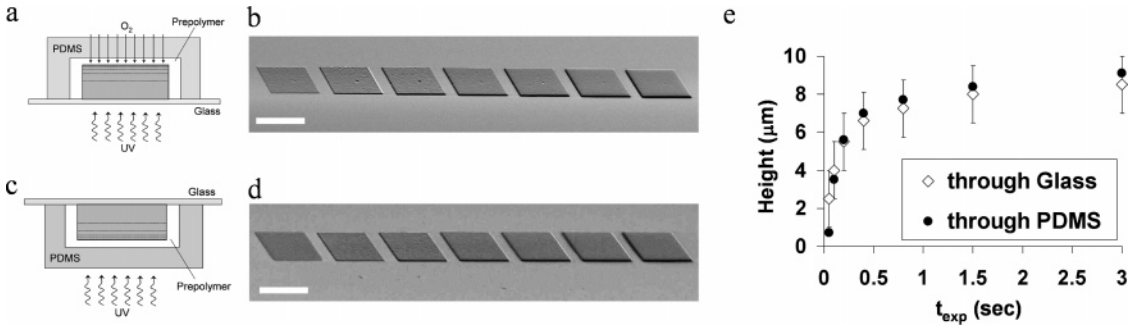

Figure 2. Variation of structure height with exposure dose when UV irradiated through the glass substrate (a, b) or PDMS channel (c, d). (a, c) Schematic of hydrogel polymerization through the glass substrate or PDMS channel. (b, d) Scanning electron micrograph of PEG structures polymerized for 0.05, 0.1, 0.2, 0.4, 0.8, 1.5, and 3 s in a 9.6-μm-tall channel. (e) Graph showing structure height with varying UV exposure times, estimated from SEM images shown in b and d. The height measurement uncertainty (shown as error bars in e) is due to the SEM image resolution (pixel size). Scale bars are 200 μm.

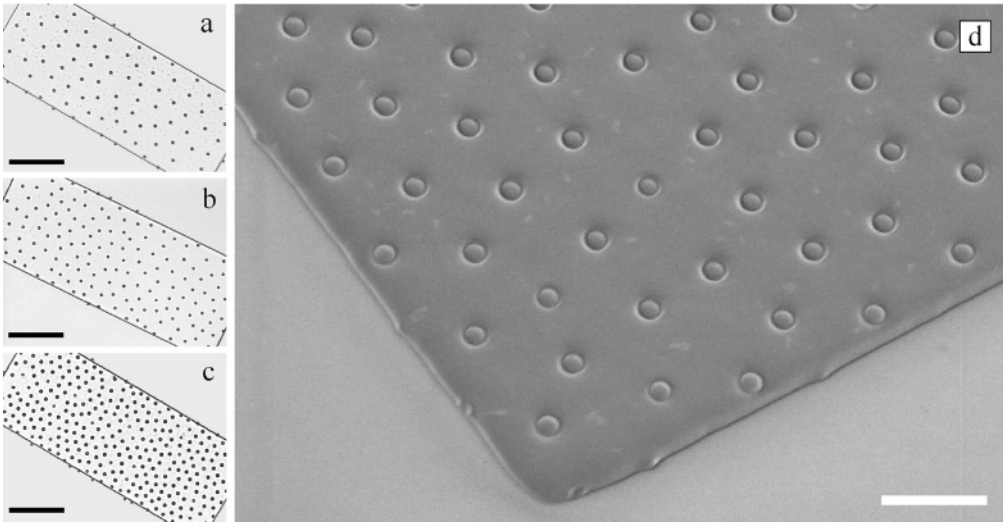

Figure 3. Dispersed magnetic bead patterns in rectangular PEG structures. (a−c) Bright-field images of PEG structures with varying concentrations of beads. (d) Scanning electron micrograph of the structure shown in c. Scale bars are 100 (a−c) and 20 μm (d).

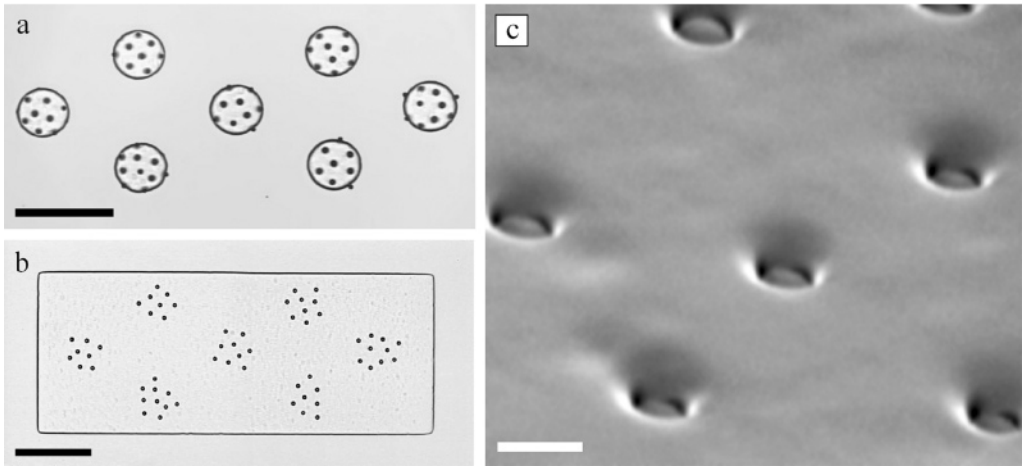

Figure 4. (a) Bright-field image of magnetic bead islands polymerized to a glass substrate. (b) Composite structure with a PEG rectangle polymerized around the magnetic bead islands. (c) Scanning electron micrograph of exposed beads in the PEG structure. Scale bars are 100 (a, b) and 5 μm (c).

The structures were then rinsed thoroughly with deionized water and dried under argon. The rectangular shapes that we polymerized were approximately 200 × 500 μm^2. By adjusting the concentration of microbeads in the prepolymer solution, we were able to tune the spacing between patterned beads (approximately 53, 40, and 28 μm) as shown in Figure 3.

We also fabricated composite pattern structures with pads of dispersed beads in rectangular PEG platforms as shown in Figure 4. Circular pads of dispersed beads were polymerized as previously described for 0.5 s. We then rinsed excess polymer from the slide, dried the pattern under argon, and placed a clean 9.6-μm-tall channel over the pattern. The channel was filled

with a bead-free prepolymer solution. We changed the mask in the microscope and polymerized a rectangular structure around the magnetic bead pads for 2 s.

Packed-Bead Magnetic Patterns. Close-packed bead patterns were generated using a protocol slightly different from that used for the dispersed bead patterns. To create a tightly packed array of microbeads, it is essential to use a channel whose height is only slightly greater than a bead diameter and that has a constriction small enough to impair bead passage. Instead of designing multi-tiered microchannels for this purpose, we simply polymerized a small slug of prepolymer in a 6.1-μm-tall channel to block the bead flow. As previously mentioned, the gel does not polymerize all the way to the PDMS surface, leaving room for fluid flow while blocking the beads from passing.

With the constriction in place, we flowed a solution of Dynabeads in 1% surfactant (in deionized water) through the channel using suction from a syringe. Once the wide region of the channel was loosely packed with beads, we placed the device directly on top of the water bath of an ultrasonic cleaner for 3 s to facilitate the close packing of beads within the channel. We then removed excess fluid from the reagent well and added our prepolymer solution (2.5% HHEMPP/1% Tergitol NP-10/96.5% PEG-DA), filling in the void space between the packed beads. As before, we polymerized mask-defined patterns for 0.5−3 s, removed the PDMS channel, rinsed the patterns with deionized water, and dried the substrate under argon. If desired, we placed a 9.6-μm-tall channel over the bead pattern and polymerized the PEG structures around the bead patterns as described before.

Using a narrow, 5-μm-wide PDMS channel, we have also demonstrated the ability to pattern a single rail of magnetic beads totally encapsulated in PEG. When polymerizing such small structures, it was necessary not only to use a high concentration of photoinitiator but also to soak the PDMS channel in a 0.1 g/mL solution of 1-hydroxycyclohexyl phenyl ketone photoinitiator (Aldrich) for 10 min prior to use. Examples of the various packed-bead patterns that we have generated are shown in Figure 5.

Exposed versus Encapsulated Bead Patterns. As mentioned, we have fabricated both exposed and PEG-encapsulated bead patterns. UV radiation cannot penetrate the magnetite-loaded microbeads because of their high opacity. The beads act as masks, preventing the monomer from polymerizing on the side of the beads opposite to the light source. Exposed-bead patterns are desirable when patterning surface-active beads. Conversely, patterns encapsulated in thin PEG films may be more useful when exploiting the beads solely for their magnetic properties while avoiding nonspecific protein and cell adhesion. To generate PEG-encapsulated bead patterns, we simply inverted the device and polymerized the PEG structures through the PDMS channel. When generating encapsulated patterns, we used channels made from thin slabs (∼1 mm) of PDMS to fit within the working distance of the microscope objective. From our experience, thinner slabs of PDMS also provided the highest-fidelity structures. Figure 6 shows beads patterned to a glass substrate with the subsequent polymerization of PEG around the bead cluster from below and above the structure.

Protein-Bound Bead Patterns. All of the aforementioned structures generated using magnetic microbeads can also be fabricated using protein-decorated beads with slight variations of the reagents used. First, it is very important to use Tween-20 or another biofriendly, nonionic surfactant in all processing steps. The proteins bound to the microbeads tend to stick to the methacrylate-modified glass surface in the absence of surfactant. The surfactant appears to protect the proteins during processing,

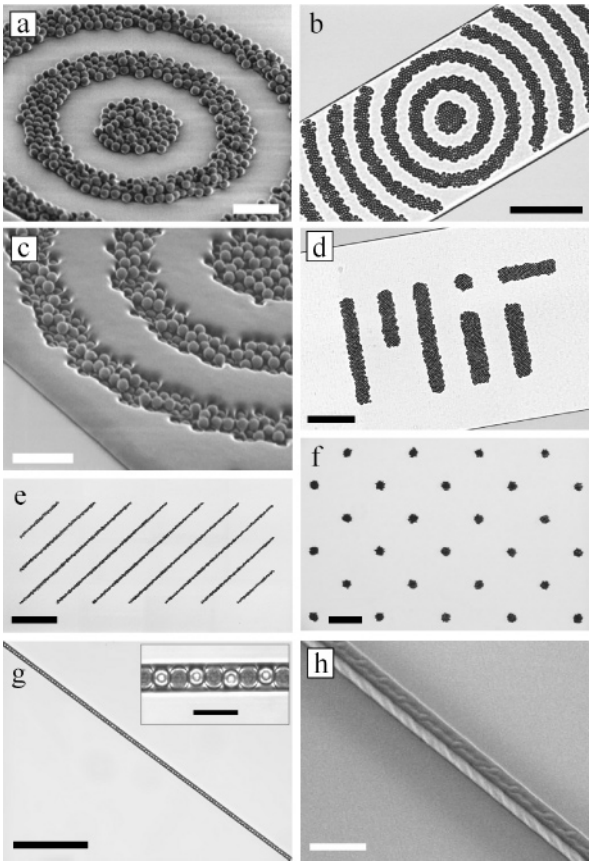

Figure 5. (a) Scanning electron micrograph of magnetic beads patterned in a target shape on a glass substrate. (b) Bright-field image and (c) scanning electron micrograph of a target bead pattern with a rectangular PEG structure polymerized around it from below the substrate. (d) Bright-field image of another packed-bead pattern with a rectangular PEG film polymerized around it. (e) Lines and (f) dots patterned to glass over lengths greater than 1 mm. (g) Bright-field image with close-up inlay of a single rail of magnetic beads encapsulated in PEG. (h) Scanning electron micrograph of the rail in g, showing that the beads are completely encapsulated in PEG. Scale bars are 20 (a, c), 100 (b, d, f, g), 200 (e), and 10 μm (g inlay, h).

helping retain protein activity while patterning. The prepolymer solution we used when patterning the anti-CD19-coated microbeads was 1.67% HHEMPP/33.3% PBS/65% PEG-DA. The dilution of prepolymer with PBS, like the addition of surfactant, appeared to help maintain the stability of the protein during the polymerization process. In addition to these alterations, we also flushed the channel with 10% BSA in PBS prior to removing the channel after pattern polymerization. We rinsed the patterns with water, and while they were still wet, added a few microliters of 30% glycerol atop the wet pattern. The glycerol protected the proteins from drying, which is known to compromise protein function.[38]

For many applications, it is desirable to capture multiple specific cell types or proteins in well-defined patterns. Bead-patterned hydrogels containing several chemically unique beads may provide an efficient, inexpensive platform to accomplish this. The patterning of diverse microbeads can be acheived by either (1) sequentially immobilizing pads of beads in a composite pattern similar to that shown in Figure 4, (2) patterning beads in adjacent channels (each filled with a unique bead type), or (3) mixing bead types (potentially fluorescently barcoded for later identi-

(38) Prestrelski, S. J.; Tedeschi, N.; Arakawa, T.; Carpenter, J. F. *Biophys. J.* **1993**, *65*, 661−671.

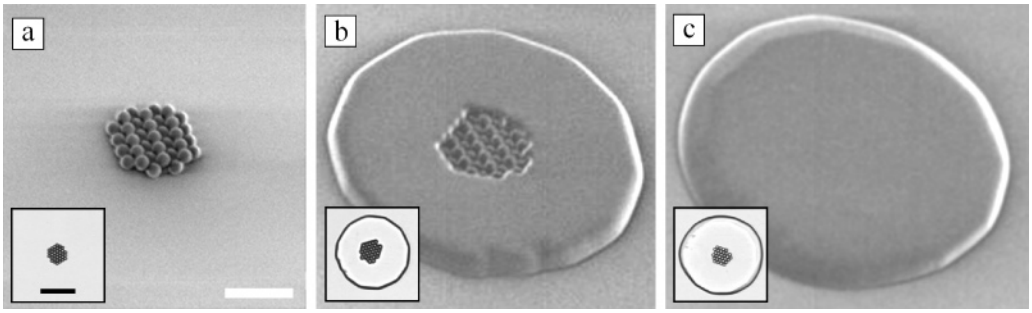

Figure 6. Scanning electron micrographs of (a) a free-standing packed-bead cluster polymerized to glass, (b) a cluster with outer PEG structure polymerized from below the glass substrate, and (c) a cluster with outer PEG structure polymerized through the PDMS channel, each with bright-field image inlays. Scale bars are 20 (a−c) and 50 μm (a−c inlays).

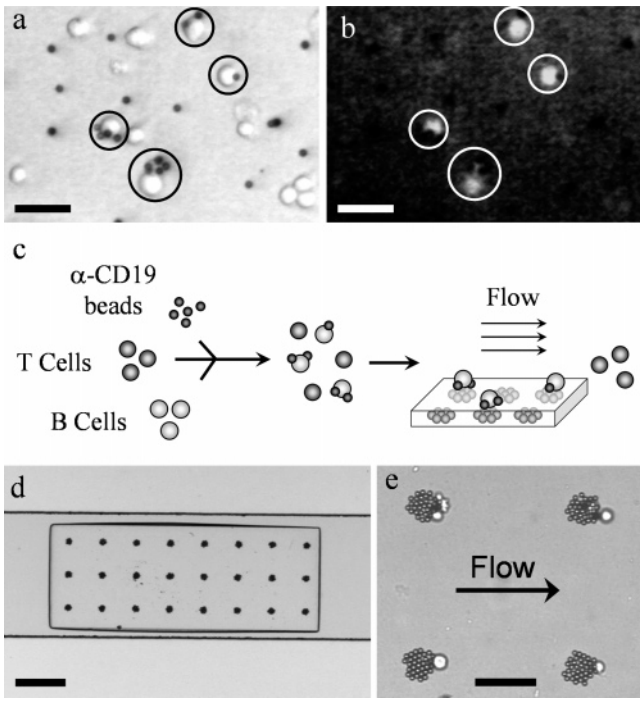

Figure 7. (a) Bright-field images of B and T cells incubated with α-CD19-decorated microbeads (with bead-bound cells circled). (b) Fluorescence image of cells in a, showing the specificity of the beads for the fluorescently dyed B cells. (c) Schematic of the magnetic-bound cell capture experiment. (d) Bright-field image of the PEG-encapsulated magnetic bead cluster platform in a microchannel. (e) Bead-bound B cells captured over the magnetic pads in a flow. Scale bars are 30 (a, b), 200 (d), and 50 μm (e).

fication) into the oligomer solution and generating chemically randomized bead patterns.

Cell Capture Experiments. To demonstrate the utility of our patterning method, we fabricated microfluidic devices to (1) capture magnetic-bound cells on bioinert magnetic pads and (2) directly capture cells on patterned, antibody-decorated beads. The patterns we generated are by no means optimized for these applications but were used solely to show the exploitation of the magnetic and bioactive nature of two bead-patterned hydrogels. The cellular specificity of immunomagnetic microbeads has been well documented[39] and is not emphasized in our experiments. We simply demonstrated selective binding of the beads to targeted B cells as shown in Figure 7a.

Capture of Magnetic-Bound B Cells. We patterned PEG-encapsulated clusters of magnetic beads to filter magnetic-bound B cells from T cells. An encapsulated pattern was used to deter

(39) Thiel, A.; Scheffold, A.; Radbruch, A. *Immunotechnology* **1998**, *4*, 89−96.

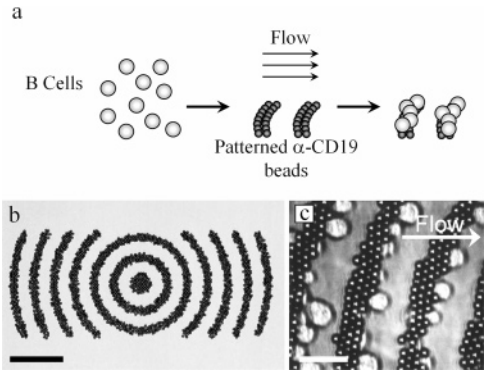

Figure 8. (a) Schematic of the direct cell capture experiment. (b) Bright-field image of patterned anti-CD19 microbeads on a glass substrate. (c) Cells captured directly on the patterned beads in a fluid flow. Scale bars are 100 (b) and 25 μm (c).

nonspecific cell adhesion to the epoxy (glycidyl ether) magnetic bead surfaces. The microfluidic device we constructed consisted of a long, 500-μm-wide, 75-μm-tall microchannel aligned over the PEG-encapsulated bead pattern. We positioned a circular electromagnet about the device, using a power source to control the current and hence the magnetic field generated. We incubated Raji B cells and Molt-3 T cells with Dynabeads CD19 as recommended by the bead supplier for 10 min. After flushing the channel for 20 min with 10% BSA solution, the cell mixture was flowed through the channel. With a magnetic field strength of ∼20 mT, we were able to capture bead-bound B cells over the patterned magnetic clusters as shown in Figure 7. The magnetic-bound cells were released into the flow when the magnetic field was turned off.

Direct Capture of B Cells on Patterned Beads. Using the protein-friendly protocol previously described, we patterned anti-CD19 beads directly onto a glass substrate in an arbitrary target shape. We aligned a 1-mm-wide, 50-μm-tall PDMS microchannel over the pattern and flushed it with 10% BSA for 20 min. We flowed a solution of B cells in through the device, capturing the cells directly on the bead patterns as shown in Figure 8. The cells adhered very well to the patterns and remained attached even under considerable shear stress. It appears as though very little protein functionality was lost in the bead-patterning process.

The intent of this experiment was to show that the antibodies conjugated to the surface of the beads maintained activity through what might seem to be a harsh process with high-intensity UV exposure, free-radical formation, exposure to a hydrophobic photoinitiator, and so forth. We are not suggesting (or denying) that this method is superior to systems that utilize surface patterning for the specific application of cell capture, but we used this scenario as a proof-of-principle. We emphasize that for certain biological applications the use of patterned beads may

have advantageous features including three-dimensionality and ultrasmall antibody spotting. The spherical nature of the beads provides a higher protein density per planar area than flat surfaces and a "bumpy" contour that might promote better interaction between flowing cells and the antibody-decorated substrate. In addition, the use of monodisperse, antibody-decorated beads provides a means to make very small (<5 μm) homogeneous spots of various chemistries. This is very difficult to achieve using traditional approaches and may be useful when fabricating protein or DNA arrays.

Conclusions

We have developed a new method to pattern magnetically active, protein-decorated microbeads on glass substrates or in bioinert PEG platforms for use in microfluidic separations. The process is fast, inexpensive, and versatile and shows potential for applications in cell sorting, generating protein or nucleic acid microarrays, and patterning biosensor arrays. We have exploited PEG-encapsulated magnetic patterns to filter bead-bound B cells from T cells and also directly captured B cells on exposed bead patterns.

Acknowledgment. We gratefully acknowledge support from the National Science Foundation (grant CTS-0304128) and the Dumbros Fellowship. We also thank Jesse Lee for his assistance during the early stages of this project.

LA0534625